Global and Stochastic Analysis
Vol. 13 No. 4 (2026)

DOI: 10.64837/GSA.13.4.11

LOEWNER ANALYSIS OF EXPERIMENTAL ISOLINES OF A FREE LIQUID SURFACE IN A TURBULENT REGIME

M. D. ZOTOV

Abstract. We analyze experimental isolines of a free liquid surface in a turbulent wave regime by means of inverse Loewner evolution. The isolines were extracted from diffuse-photography images and divided into chord-length-normalized fragments. For seven experiments containing 525000 contour points and 1050 fragments, the reconstructed driving functions show a nonzero mean drift and a variance growth that is not Brownian. The empirical variance is described by the power law $\mathrm{Var}(W_t) \sim t^{\alpha}$ with $\alpha = 1.53 \pm 0.09$, giving $H = 0.763 \pm 0.045$. The observed isolines are therefore not classical SLE curves. They are more accurately described as Loewner curves with correlated and drifting driving functions.

1. Introduction

Turbulence is usually described in terms of velocity fields, correlation functions, structure functions, and energy spectra. In the Kolmogorov picture, energy injected at large scales is transferred through an inertial range and dissipated at small scales [7, 8, 4]. This description is primarily spectral, but turbulent systems also possess a nontrivial geometry. Interfaces, fronts, vortex boundaries, and level lines of physical fields may display scale-dependent irregularity, and this geometry can provide information complementary to conventional spectral characteristics [10].

A free liquid surface in a turbulent wave regime is a natural object for such a geometrical analysis. Let $h(x, y, t)$ be the instantaneous surface-height field. The curves

$$h(x, y, t) = h_0 \tag{1.1}$$

are planar random curves, where h_0 is a fixed reference level, for instance the level of the unperturbed surface. These curves encode the spatial organization of the wave field and may reflect the scale structure of the turbulent regime.

A powerful method for analyzing random planar curves is the Loewner evolution. In this approach, the geometry of a growing curve in a simply connected planar domain is encoded by a one-dimensional real-valued driving function. In the special case of Schramm–Loewner evolution (SLE), the driving function is

---

Date: Date of Submission 16th May 2026; Date of Acceptance 1 July 2026, Communicated by Yuri E. Gliklikh.

2010 *Mathematics Subject Classification.* Primary 60J67; Secondary 76F55, 76B15, 30C35.

Key words and phrases. Loewner evolution, Schramm–Loewner evolution, turbulent surface waves, driving function, anomalous scaling, diffuse photography.

Brownian motion with diffusivity κ [13, 9, 3, 5]. Reconstructing the driving function from experimental curves therefore provides a direct test of SLE-like behavior. Related ideas have been used in the analysis of random geometry in turbulent and statistical systems [2].

The aim of this work is to apply inverse Loewner evolution to experimentally obtained isolines of a turbulent free surface. Unlike an ideal theoretical SLE curve, an experimental curve may contain anisotropy, finite-size effects, drift, correlated increments, and image-processing noise. Therefore we do not assume in advance that the curves are classical SLE curves. Instead, the Loewner transform is used as a diagnostic tool: the reconstructed driving functions are tested for Brownian scaling, drift, and power-law variance growth.

The main observation is that the turbulent surface isolines demonstrate SLE-like geometry only in a restricted effective sense. A linear fit of the driving-function variance gives a finite formal parameter κ_{lin}, but the variance is described more accurately by a superdiffusive power law. Thus the reconstructed driving function contains memory, and the curves should be regarded as Loewner curves with correlated and drifting driving functions rather than as classical SLE curves.

2. Loewner Evolution and Experimental Criteria

2.1. Chordal Loewner equation. Consider a simple curve $\gamma[0, t]$ growing in the upper half-plane $\mathbb{H}$ from a point on the real axis. The domain $\mathbb{H} \setminus \gamma[0, t]$ is mapped conformally back to $\mathbb{H}$ by a function $g_t(z)$

$$g_t(z) = z + \frac{2t}{z} + O(z^{-2}), \qquad z \to \infty. \tag{2.1}$$

The parameter t is the half-plane capacity, or Loewner time. The chordal Loewner equation is

$$\frac{dg_t(z)}{dt} = \frac{2}{g_t(z) - W_t}, \tag{2.2}$$

where W_t is a real-valued driving function. This function contains the information about the shape of the curve [11].

For Schramm–Loewner evolution,

$$W_t = \sqrt{\kappa}\, B_t, \tag{2.3}$$

where B_t is standard Brownian motion. Consequently,

$$\mathbb{E}W_t = 0, \qquad \mathrm{Var}(W_t) = \kappa t. \tag{2.4}$$

The linear growth of variance is the main Brownian criterion for classical SLE. If one formally projects experimental data onto this form, the slope gives an effective parameter κ_{lin}. For $\kappa \le 8$, the SLE fractal dimension is

$$D_f = 1 + \frac{\kappa}{8}. \tag{2.5}$$

In the present work this relation is used only as an effective geometrical comparison, because the Brownian criterion itself is tested from the data.

2.2. Discrete inverse Loewner evolution. The experimental curve is represented by a finite sequence of points

$$z_i = x_i + iy_i, \qquad i = 0, 1, \ldots, N. \tag{2.6}$$

To reconstruct the driving function, we use a discrete inverse Loewner procedure based on the vertical-slit approximation. At each step the current first point of the curve is interpreted as the tip of a small vertical slit. The corresponding conformal map is

$$g_{\Delta t_i}(z) = \sqrt{(z - W_i)^2 + 4\Delta t_i}, \tag{2.7}$$

where

$$W_i = x_i, \qquad \Delta t_i = \frac{y_i^2}{4}. \tag{2.8}$$

After applying the map to all remaining points, the next point becomes the new tip. Repeating the procedure gives a discrete driving function $W(t_n)$ with

$$t_n = \sum_{i=1}^{n} \Delta t_i. \tag{2.9}$$

Before reconstruction, each curve fragment is translated, rotated, and rescaled so that its initial point is at the origin and the chord between the first and last points lies along the real axis. In complex notation the normalization is

$$z_i \mapsto \frac{(z_i - z_0)e^{-i\arg(z_N - z_0)}}{|z_N - z_0|}. \tag{2.10}$$

This step is essential for comparing different fragments, because under the scaling $z \mapsto z/L$ one has $W \mapsto W/L$ and $t \mapsto t/L^2$.

3. Experimental Data and Processing

The isolines were obtained from images of a free liquid surface recorded by diffuse photography. The experiment used a transparent container with a working area of approximately $500 \times 750\,\mathrm{mm}^2$ and an unperturbed liquid depth of approximately 7 cm. Surface waves were generated by a circular mechanical exciter of diameter about 150 mm with holes of different sizes. Such forcing produces an inhomogeneous wave field with a broad range of spatial scales.

The working fluid was a weak aqueous milk solution. Milk particles increase light scattering, so that the intensity recorded by the camera depends on the local optical path length through the liquid. Surface-height variations therefore produce intensity variations. After background subtraction and filtering, level lines corresponding to the chosen reference surface level were extracted.

The processing pipeline is summarized in Fig. 1. It consisted of image registration, background subtraction, filtering and thresholding, contour extraction, ordering of contour points, splitting long curves into fragments of length 500 points, applying the normalization above, and reconstructing $W(t)$ by the inverse Loewner procedure.

The main statistical analysis was performed for seven experiments, denoted by indices $0, \ldots, 6$. In total, they resulted in 525000 contour points and 1050 fragments of length 500. For each fragment a driving function was reconstructed

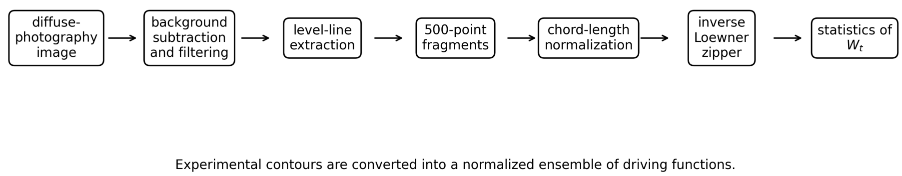

FIGURE 1. Processing pipeline used to convert diffuse-photography images into an ensemble of normalized Loewner driving functions.

and then interpolated onto a common Loewner-time grid. Ensemble averages were computed over all fragments belonging to the same experiment and over the full set of experiments.

4. Statistical Quantities

For each reconstructed driving function, we analyze three quantities. The first is the ensemble mean

$$\langle W_t \rangle. \tag{4.1}$$

If the curves were exactly described by classical chordal SLE in the chosen normalization, this mean would vanish. In the experimental data it is useful to approximate it by a linear drift

$$\langle W_t \rangle \simeq vt. \tag{4.2}$$

The coefficient v characterizes a systematic directed component of the driving function.

The second quantity is the variance

$$\mathrm{Var}(W_t) = \left\langle (W_t - \langle W_t \rangle)^2 \right\rangle. \tag{4.3}$$

The Brownian SLE criterion corresponds to the linear law

$$\mathrm{Var}(W_t) = \kappa t. \tag{4.4}$$

We also fit the more general power law

$$\mathrm{Var}(W_t) = At^{\alpha}. \tag{4.5}$$

If $\alpha = 1$, the scaling is Brownian. If $\alpha > 1$, the driving function is superdiffusive. It is then useful to write

$$\alpha = 2H, \tag{4.6}$$

where H is the Hurst exponent. Brownian motion has $H = 1/2$, while $H > 1/2$ indicates persistent correlations in the increments.

5. Results

Figure 2 shows a sample of reconstructed driving functions for the first experiment. The functions are not identical, but their ensemble statistics reveal a clear systematic behavior.

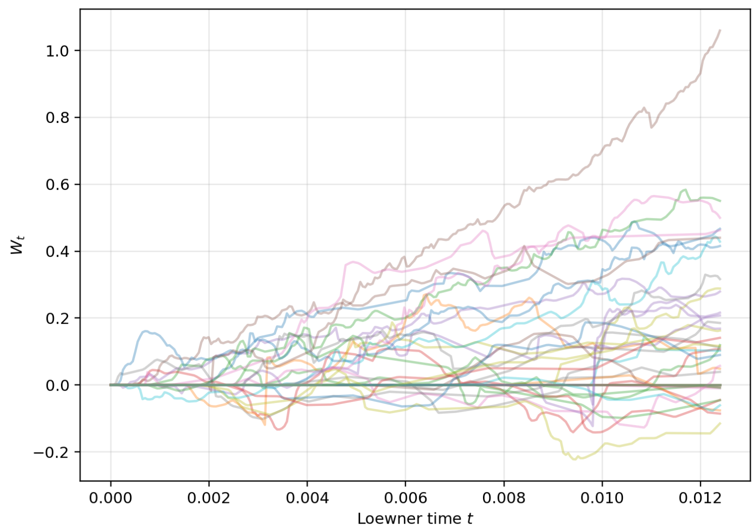

FIGURE 2. Sample of reconstructed Loewner driving function.

For each set of curves we estimated the linear slope $\kappa_{\rm lin}$, the formal SLE dimension $D_f = 1 + \kappa_{\rm lin}/8$, the power-law exponent α, the Hurst exponent $H = \alpha/2$, and the drift coefficient v. The results are listed in Table 1.

TABLE 1. Loewner statistics for the seven main experiments.

№	$\kappa_{\rm lin}$	D_f	α	H	v
0	2.817	1.352	1.656	0.828	11.257
1	2.722	1.340	1.558	0.779	11.089
2	2.830	1.354	1.522	0.761	9.240
3	2.651	1.331	1.577	0.789	9.702
4	1.936	1.242	1.364	0.682	7.986
5	2.890	1.361	1.520	0.760	9.447
6	2.273	1.284	1.481	0.740	7.788

The mean values and 95% confidence intervals for the seven-experiment ensemble are

$$\kappa_{\rm lin} = 2.59 \pm 0.35, \qquad \kappa_{\rm lin} \in [2.26, 2.91], \tag{5.1}$$
$$D_f = 1.324 \pm 0.044, \qquad D_f \in [1.283, 1.364], \tag{5.2}$$
$$\alpha = 1.53 \pm 0.09, \qquad \alpha \in [1.442, 1.609], \tag{5.3}$$
$$H = 0.763 \pm 0.045, \qquad H \in [0.721, 0.804], \tag{5.4}$$
$$v = 9.50 \pm 1.35, \qquad v \in [8.25, 10.75]. \tag{5.5}$$

Here the uncertainties after the $\pm$ sign are sample standard deviations over the seven experiments, while the intervals give the corresponding 95% confidence intervals for the mean.

Figure 3 shows the exp.-to-exp. variability of $\kappa_{\rm lin}$ and α. The effective linear parameter remains in a moderate range, while the exponent α is consistently larger than one.

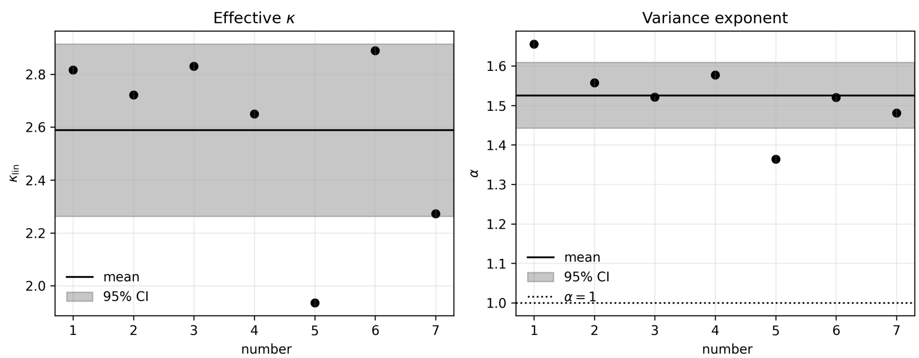

FIGURE 3. Values of the effective linear parameter $\kappa_{\rm lin}$ and the variance exponent α. Horizontal lines show ensemble means and shaded regions show 95% confidence intervals for the mean. The dotted line in the right panel marks the Brownian value $\alpha = 1$.

The difference between the Brownian and anomalous descriptions is visible directly in the variance. Figure 4 shows the variance and the mean driving function for the first experiment. The variance is fitted both by a linear law and by a power law, while the mean driving function displays a robust approximately linear drift.

6. Discussion

The reconstructed driving functions do not satisfy the strongest criterion for classical SLE. For SLE, the driving function must be Brownian: its mean must vanish, its variance must grow linearly with Loewner time, and its increments must be independent. The experimental data show a different pattern. The variance grows as a power law with exponent significantly larger than one, and the mean driving function contains a systematic drift.

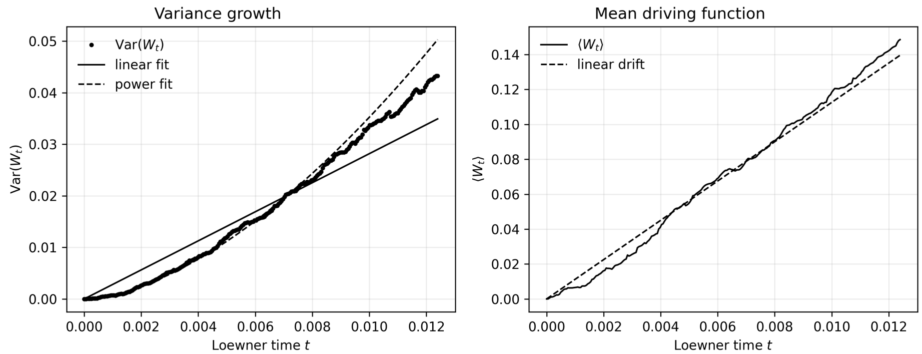

FIGURE 4. Example of the reconstructed driving-function statistics for first experiment. Left: variance growth with linear and power-law fits. Right: mean driving function and linear drift fit.

This distinction changes the interpretation of the Loewner analysis. The purpose of the reconstruction is not to force the experimental curves into a Brownian SLE class. Instead, the Loewner transform reduces each planar isoline to a one-dimensional driving process whose statistics can be measured directly. In this representation the main experimental signatures are

$$\alpha \approx 1.53, \qquad H \approx 0.76, \qquad v \approx 9.50. \tag{6.1}$$

The value $\alpha > 1$ indicates superdiffusive growth of the driving-function variance. Equivalently, $H > 1/2$ indicates persistent correlations: increments of the driving function tend to keep the same sign more strongly than in Brownian motion.

The observed drift has a separate physical meaning. It may arise from anisotropy of the mechanical forcing, from the finite geometry of the container, from a preferred direction introduced by the extraction of curve fragments, or from residual asymmetry in the image-processing procedure. In an ideal SLE ensemble such a drift is absent, so its observation is another reason not to interpret the curves as classical SLE curves.

The result is consistent with the nature of the experiment. Turbulent surface waves are not generated by an equilibrium conformally invariant lattice model. They are produced by mechanical forcing in a finite container and are affected by dissipation, boundary conditions, finite imaging resolution, and the dynamics of the liquid surface. Exact conformal invariance should therefore not be expected. What the experiment reveals is a more general Loewner-type random geometry with memory and anisotropy.

From this viewpoint, the important output of the method is the set of measured driving-function statistics, rather than a single effective SLE diffusivity. The inverse Loewner transform is useful precisely because it shows where the classical SLE picture breaks down and replaces it with quantitative characteristics of the experimental curves.

7. Conclusion

We analyzed experimental isolines of a free liquid surface in a turbulent wave regime using inverse Loewner evolution. The isolines were extracted from diffuse-photography images and split into fragments of length 500 points. For seven experiments, resulting in 525000 contour points and 1050 fragments, driving functions were reconstructed and statistically analyzed.

The reconstructed driving functions do not satisfy the Brownian criterion of classical SLE. A linear projection of the variance gives an effective value $\kappa_{\text{lin}} = 2.59 \pm 0.35$ and a formal dimension $D_f = 1.324 \pm 0.044$, but the more informative result is the anomalous scaling

$$\text{Var}(W_t) \sim t^{\alpha}, \qquad \alpha = 1.53 \pm 0.09. \tag{7.1}$$

The associated Hurst exponent is

$$H = 0.763 \pm 0.045, \tag{7.2}$$

which indicates persistent correlations in the reconstructed driving function. A systematic drift,

$$v = 9.50 \pm 1.35, \tag{7.3}$$

is also observed in the chord-length-normalized ensemble.

Thus, the experimental curves should not be interpreted as classical SLE curves and should not be characterized primarily by an effective Loewner diffusivity. A more accurate statement is that turbulent free-surface isolines generate non-Brownian Loewner driving functions with anomalous variance growth, persistent correlations, and drift. The Loewner transform is therefore useful as a diagnostic tool for detecting memory and anisotropy in experimental random curves.

References

[1] Bauer, M., Bernard, D.: Conformal field theories of stochastic Loewner evolutions, *Comm. Math. Phys.*, 239, 2003, 493–521.

[2] Bernard, D., Boffetta, G., Celani, A., Falkovich, G.: Conformal invariance in two-dimensional turbulence, *Nature Phys.*, 2, 2006, 124–128.

[3] Cardy, J.: SLE for theoretical physicists, *Ann. Phys.*, 318, 2005, 81–118.

[4] Frisch, U.: *Turbulence: The Legacy of A. N. Kolmogorov*, Cambridge University Press, Cambridge, 1995.

[5] Kager, W., Nienhuis, B.: A guide to stochastic Loewner evolution and its applications, *J. Stat. Phys.*, 115, 2004, 1149–1229.

[6] Kennedy, T.: A fast algorithm for simulating the chordal Schramm–Loewner evolution, *J. Stat. Phys.*, 128, 2007, 1125–1137.

[7] Kolmogorov, A. N.: The local structure of turbulence in incompressible viscous fluid for very large Reynolds numbers, *Dokl. Akad. Nauk SSSR*, 30, 1941, 301–305.

[8] Kolmogorov, A. N.: Dissipation of energy in locally isotropic turbulence, *Dokl. Akad. Nauk SSSR*, 32, 1941, 16–18.

[9] Lawler, G. F.: *Conformally Invariant Processes in the Plane*, American Mathematical Society, Providence, 2005.

[10] Mandelbrot, B. B.: Intermittent turbulence in self-similar cascades: divergence of high moments and dimension of the carrier, it J. Fluid Mech., 62, 1974, 331–358.

[11] Marshall, D. E., Rohde, S.: The Loewner differential equation and slit mappings, *J. Amer. Math. Soc.*, 18, 2005, 763–778.

[12] Rohde, S., Schramm, O.: Basic properties of SLE, *Ann. of Math.*, 161, 2005, 883–924.

[13] Schramm, O.: Scaling limits of loop-erased random walks and uniform spanning trees, *Israel J. Math.*, 118, 2000, 221–288.

South Ural State University, Chelyabinsk, Russia
Email address: zotov.fml@gmail.com